Inorganic Chemistry

Communication

pubs.acs.org/IC

Open-Shell Triplet Character of $^{\#6094}C_{68}$: Spherical Aromaticity, Thermodynamic Stability, and Regioselective Chlorination

Jing-Shuang Dang, Jia-Jia Zheng, Wei-Wei Wang, and Xiang Zhao*

Institute for Chemical Physics and Department of Chemistry, Xi'an Jiaotong University, Xi'an, China

Supporting Information

ABSTRACT: The recently captured fullerene $^{\#6094}C_{68}$ was found to exhibit a more aromatic character than originally assumed via density functional theory calculations. Such an inconsistency was attributed to the unexpected triplet ground state of pristine $^{\#6094}C_{68}$. The equilibrium concentrations of C_{68} isomeric system reveal that $^{\#6094}C_{68}$ is thermodynamically favorable at elevated temperatures with respect to the fullerene formation. The regioselective chlorination process of the open-shell C_{68} was discussed as well to elucidate the formation of octachlorinated derivative $C_{68}Cl_8$ experimentally.

Aromaticity has thus far served as a fundamental criterion in predicting the physicochemical properties of cyclic hydrocarbons.[1,2] In particular, Hirsch's $2(N + 1)^2$ rule for closed-shell spherical compounds as well as Solà's $2N^2 + 2N + 1$ (with a spin of $S = N + {}^1/_2$) rule for open-shell spherical species were put forward to estimate the aromatic character of fullerenes with a delocalized π system.[3,4] Among various theoretical criteria of aromaticity, the calculated nucleus independent chemical shift (NICS) has been widely employed to evaluate the aromatic properties of nonplanar fullerene structures.[5] Generally, a more negative NICS value at the cage center represents more aromatic character of the fullerene molecule.[5] To date, the neutral hollow fullerenes with positive NICS values have never been observed experimentally, implying that the aromatic rule should be reliable in estimating the stability of fullerenes.

Recently, by in situ chlorination in the radio-frequency furnace, a C_s-symmetric C_{68} isomer (denoted as $^{\#6094}C_{68}$ by Fowler's spiral algorithm[6]) with two pentagon pairs was captured as a chloride $C_{68}Cl_8$.[7] The authors also performed theoretical calculations, which indicated this isomer had a novel positive NICS (22.47 ppm, at the B3LYP/6-311G level of theory), and suggested that this was the first experimental evidence of the antiaromatic pristine fullerenes.[7] Unfortunately, although this structure has been characterized by means of mass spectrometry and single-crystal X-ray diffraction, the conclusion in that literature may be misleading because of an evident negligence of their theoretical calculations. In the above-mentioned report and some previous theoretical investigations,[7−9] $^{\#6094}C_{68}$ was predicted as a novel antiaromatic molecule because of the positive NICS value. However, all of those calculations were performed with the closed-shell singlet and no other spin states were considered. It is known that the spin behavior of electrons determines the stability, magnetoelectronics, and chemical reactivity of a molecule. Therefore, it is apparent that the precondition of analyses on all sorts of properties is to find the correct electronic ground state. Actually, $^{\#6094}C_{68}$ was mentioned as a triplet fullerene by Tan et al. when they discussed the relative energies of C_{68} isomers,[10] so there is no doubt that the effect of the spin state should be taken into account. Herein, on the basis of spin-restricted and spin-unrestricted density functional theory (DFT) calculations, the energies, thermodynamic stabilities, and aromatic properties of pristine $^{\#6094}C_{68}$ were refocused. Interestingly, our calculations suggest that $^{\#6094}C_{68}$ is indeed a *special* fullerene species, while the essential specificity does not lie in the so-called antiaromaticity but the open-shell ground state. Moreover, according to the unique spin character of hollow $^{\#6094}C_{68}$, chlorination on the open-shell fullerene has been evaluated for the first time by the stepwise radical mechanism. We found that the electronic spin state plays an important role in the regioselective exohedral derivatization process.

First, to verify the ground state of $^{\#6094}C_{68}$, we calculated the relative energies with different spin states at various levels of theory. As listed in Table S1 in the Supporting Information (SI), all energy calculations reveal that the ground state of $^{\#6094}C_{68}$ should be triplet rather than singlet. The singlet−triplet splitting energy ($\Delta E_{st} = E_{singlet} - E_{triplet}$) is as high as 8.2 kcal mol^{-1} at the B3LYP/6-311++G(d,p) level of theory. In order to gain deeper insight into the triplet fullerene, frontier orbital analyses of $^{\#6094}C_{68}$ were performed and the results indicate that the HOMO−LUMO gap of singlet $^{\#6094}C_{68}$ is as low as 0.65 eV, revealing that the electron transition from a closed-shell singlet to triplet state easily occurs to generate an open-shell structure. Furthermore, the energy gap of triplet $^{\#6094}C_{68}$ is up to 2.38 eV, which may account for the higher stability of the triplet carbon cage. Owing to the novel open-shell ground state, previous investigations on the stability and properties of $^{\#6094}C_{68}$ were unavoidably deviated from reality. Next, we have restudied the aromaticity and thermodynamic stability, in order to exhibit a different but authentic $^{\#6094}C_{68}$.

The discovery of open-shell aromaticity can be tracked back to Baird in 1972,[2] who proposed that the $4n\pi$-electron annulenes in the lowest triplet state are aromatic rather than antiaromatic. Then, the triplet aromaticity was confirmed by Gogonea and coworkers[11] using DFT studies. Herein, to estimate the aromatic character of the open-shell carbon cage in brief, NICS values at the center of triplet fullerene spheres were calculated at different theoretical levels, by using the gauge-including atomic orbital (GIAO) method. It should be note that NICSs performed via the GIAO approach for open-shell systems are unphysical and

Received: February 4, 2013
Published: April 17, 2013

ACS Publications © 2013 American Chemical Society

inevitably approximate because the computed values are not chemical shifts any more and the nuclei will be influenced by the electron spin, but hitherto the use of NICS is still one of the most popular and instructive measures to identify the aromaticity of open-shell structures.[4,11,12] Our calculations (Table S2, SI) indicate that $^{\#6094}C_{68}$ possesses a negative NICS value of −19.91 ppm at B3LYP/6-311++G(d,p), which is more negative than that of neutral C_{60} (−3.93 ppm) at the same level, implying that $^{\#6094}C_{68}$ exhibits triplet aromaticity in the ground state. However, the computed NICS value of C_{68} is less negative than those of C_{60}^{10+} (−81.84 ppm), which follows Hirsch's $2(N+1)^2$ rule, and the open-shell C_{60}^{-} ($S = {}^{11}/_{2}$, −31.90 ppm), which follows the $2N^2 + 2N + 1$ rule,[3,4] suggesting that C_{68} has a slightly spherical aromatic character. Moreover, the local aromaticity of each carbocyclic ring has also been calculated. In contrast to the antiaromatic singlet C_{68} with no diatropic ring,[7] the triplet cage contains diatropic hexagons with negative NICS values and paratropic pentagons with positive NICS values in the surface, indicating that C_{68} is somewhat more aromatic than originally assumed.

Besides the aromatic property, we have also investigated the role of an open-shell $^{\#6094}C_{68}$ isomer in a C_{68} isomeric system. Recently, Wang et al. proposed that a heptagon-containing C_{68} isomer captured as chloride experimentally was the most dominant structure at elevated temperatures (2000 to 2500 K) while evaluating the relative concentrations at the B3LYP/6-31G(d,p) level of theory.[13] On the contrary, the molar fraction of $^{\#6094}C_{68}$ in that report was proven to be very small, with a maximum yield of about 5% at 2500 K. In addition, the insignificant molar fraction of $^{\#6094}C_{68}$ was also mentioned by Chen et al.[8] These outcomes imply that $^{\#6094}C_{68}$ is thermodynamically unfavorable in the temperature region where fullerene formation occurs. Obviously, such a conclusion cannot be used to explain the synthesis of $^{\#6094}C_{68}$ in the radio-frequency furnace at elevated temperatures.[7] Similar to the estimation on the aromatic property, the imperfect computation approach without consideration of the triplet state may give rise to an incorrect evaluation on the thermodynamic stability of $^{\#6094}C_{68}$. Hence, in the present work, we restudied the equilibrium concentrations of C_{68} set in order to get a more reasonable theoretical explanation of the experimental evidence.

Like those employed in ref 13, 15 isomers were selected in this work, among which there are 9 classical isomers and 6 nonclassical ones with heptagonal rings. These isomers were coded as idX from the GSW heuristic program,[14] and the corresponding geometric coordinates are given in the SI (Tables S3−S17). For convenience, the corresponding spiral code (#M, where M = spiral label) for each classical C_{68} species was also represented. For example, the GSW code of $^{\#6094}C_{68}$ is id144, so this isomer is labeled as id144(#6094) in the following. Optimizations on each isomer at singlet, triplet, and quintet were performed at the B3LYP/6-31G(d,p) level of theory. Similar to the results by Tan and coauthors at the PBE/DNP level of theory,[10] our calculations (Table S18, SI) indicate that id144(#6094) and id87(#6146) are the only two species with a triplet ground state; the splitting energies for id144 and id87 were 8.8 and 3.8 kcal mol^{-1}, repectively. On the basis of geometrical optimizations and vibrational frequency analyses, the equilibrium concentrations for these isomers were calculated in a wide temperature interval. It should be noted that the electronic partition function was considered in the present work because the small singlet−triplet splitting energies of species may influence the total distribution. As illustrated in Figure 1, in contrast with previous studies, the triplet id144(#6094) shows a

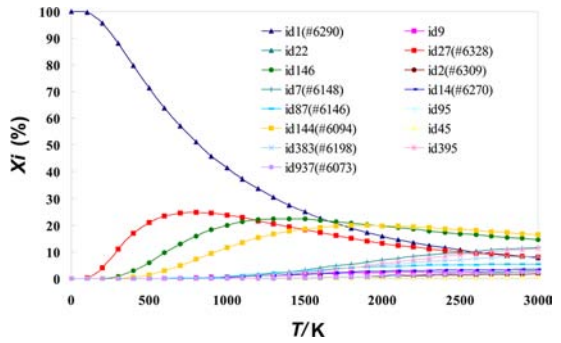

Figure 1. Relative equilibrium concentrations of C_{68} isomers at the (U)B3LYP/6-31G(d,p) level of theory.

noticeable molar fraction and becomes the most predominant isomer above 2000 K, indicating that the $^{\#6094}C_{68}$ structure is thermodynamically favorable at elevated temperatures. Furthermore, although surpassed by id144(#6094), the heptagon-incorporating id146 is still one of the two species whose ratios of molar concentrations are beyond 15% over the range of 2000−2500 K with respect to the fullerene formation. The results may give some reasonable explanation for the formation of both $^{\#6094}C_{68}$ and the nonclassical hepta-C_{68}(id146).

Because $^{\#6094}C_{68}$ was captured as chloride $C_{68}Cl_8$,[7] the chlorination mechanism has been elucidated in this work at the B3LYP/6-311G(d,p) level of theory. The Schlegel diagram of C_{68} was illustrated, and the eight chlorinated sites (C1−C8) were marked as green dots (Figure S2, SI). Fullerene chlorination occurring at higher temperatures has been suggested to be a radical addition process.[15] Geometrically, according to the strain-relief principle,[16] the carbon atoms on the fullerene sphere with larger pyramidalization angles (π-orbital axis vector, POAV) are usually more feasible to assemble with foreign adatoms to release the structural strain.[17] Moreover, Fowler and co-workers proposed that the radical addition for a closed-shell molecule always occurs on the site with the highest free-valence index and the atomic contribution of HOMO was used to represent the reactivity of each atom.[18] Furthermore, in the case of open-shell molecules with unpaired electrons, it has been demonstrated that chlorine addition prefers to take place on the site with the largest spin density to reduce the net spin.[18] Therefore, both the geometrical and electronic characteristics of $C_{68}Cl_x$ (x = 0−7) were considered to study the chlorination process.

The POAV value and the calculated spin density (for C_{68}, $C_{68}Cl_5$, and $C_{68}Cl_7$) as well as the coefficient of HOMO (for $C_{68}Cl_2$ and $C_{68}Cl_4$) of each carbon atom on the $C_{68}Cl_x$ (x = 0−7) surface are listed in Tables S19−S23 in the SI. The stepwise chlorination pathway is depicted in Figure 2, and a diagram of the spin density or HOMO distribution for each structure is drawn as well. As illustrated in Figure 2a and Table S19 in the SI, the chemically equivalent C1 and C2 atoms were considered as the first addition sites because the two identical carbon atoms exhibit the largest spin density (0.30) and the second largest POAV value (14.8°) among all 68 atoms in $^{\#6094}C_{68}$. In comparison with C1 and C2, C3 and C4 have the larger pyramidalization angles (16.3°) but hold fewer spin distributions (0.10). Similarly, C9 and C10 exhibit remarkable spin distributions (0.28) as well, but the corresponding POAV values (10.5°) are small. The relative energies of the different $C_{68}Cl_2$ are listed in Table S24 in the SI,

dx.doi.org/10.1021/ic400290a | Inorg. Chem. 2013, 52, 4762−4764

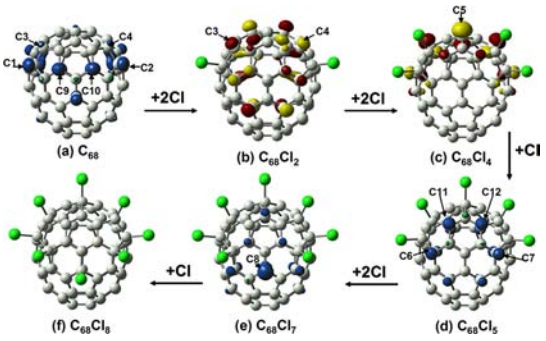

Figure 2. Chlorination pathway with diagrams of the spin density (for C_{68}, $C_{68}Cl_5$, and $C_{68}Cl_7$) or HOMO (for $C_{68}Cl_2$ and $C_{68}Cl_4$) distributions.

and the dichloride of C_{68} possessed the largest formation energy while C1 and C2 were saturated, which demonstrates that the two carbon atoms are indeed the most suitable reaction sites on the pristine C_{68} surface. Interestingly, the ground state of $C_{68}Cl_2$ in Figure 2a was singlet with a splitting energy of 34.1 kcal mol^{-1}, indicating that the two unpaired electrons were saturated by chlorination.

Subsequently, further chlorination on the closed-shell $C_{68}Cl_2$ was investigated. As shown in Figure 2b and Table S20 in the SI, owing to the largest POAV value (15.3°) and obvious coefficient in HOMO (6.7%), the two carbon atoms on the [5,5] junctions, C3 and C4, served as the reactive positions for the addition, and this corresponding tetrachlorinated $C_{68}Cl_4$ was predicted by Amsharov et al.[7] While the four atoms on the two pentagon pairs change to the sp^3-hybridized state, as seen in Figure 2c and Table S21 in the SI, C5 in $C_{68}Cl_4$ exhibits a predominant contribution of HOMO (17.5%) and a large pyramidalization angle (16.4°), so it is apparent that C5 is the fifth addition site and the corresponding adduct (see Figure 2d) is a doublet structure with odd electrons. The spin distribution and local strain for this open-shell $C_{68}Cl_5$ were evaluated (Table S22 in the SI), and the results indicate that there is not an obvious difference in POAV for each atom but the spin density is evidently distributed on the two kinds of nonequivalent carbon atoms, C6 (or C7, spin = 0.26) and C11 (or C12, spin = 0.28). Energetically, $C_{68}Cl_7$ behaves at lower energy, while C6 and C7 are selected as the addition sites (Table S25, SI); hence, the identical C6 and C7 are more suitable for the addition to generate the heptachloride of C_{68}. In the last step, as exhibited in Figure 2e and Table S23 in the SI, C8 is indubitably the most reactive carbon atom for chlorination to afford the final $C_{68}Cl_8$ product because of the unique spin density (0.47) and local strain (POAV = 13.0°). Overall, the stepwise chlorination process described above has successfully explained the formation of experimentally captured $C_{68}Cl_8$. Such an investigation may be useful in understanding the chlorination mechanism of fullerenes with unpaired electrons, such as the open-shell $^{\#1911}C_{64}$ and $^{\#4348}C_{66}$.[19] Additionally, because the C_{3v}-symmteric $^{\#1911}C_{64}$ has been identified in two forms of chlorides ($C_{64}Cl_4$ and $C_{64}Cl_8$),[20,21] the possibility of other mechanisms and other chlorinated derivatives of C_{68} cannot be excluded as well.

As a whole, DFT calculations were performed to evaluate the electronic ground state, aromatic property, thermodynamic stability, and selective chlorination process of $^{\#6094}C_{68}$. The present results may uncover the underlying characteristics of recently synthesized C_{68} and supply some valuable theoretical information to understand the special fullerenes with open-shell character.[19,22,23]

■ ASSOCIATED CONTENT

Supporting Information

Computational details, local NICS (in ppm) distributions and Schlegel diagram of $^{\#6094}C_{68}$, geometric coordinates and calculated energies of C_{68} isomers, coefficients in HOMO, POAV values, and spin densities of each carbon atom in $C_{68}Cl_n$ (n = 0−7). This material is available free of charge via the Internet at http://pubs.acs.org.

■ AUTHOR INFORMATION

Corresponding Author

*E-mail: xzhao@mail.xjtu.edu.cn. Tel: +86 29 8266 5671.

Notes

The authors declare no competing financial interest.

■ ACKNOWLEDGMENTS

This work has been supported by National Natural Science Foundation of China (Grant 21171138).

■ REFERENCES

(1) Minkin, V. I.; Glukhovtsev, M. N.; Simkin, B. Y. *Aromaticity and Antiaromaticity*; John Wiley & Sons: New York, 1994.
(2) Baird, N. C. *J. Am. Chem. Soc.* **1972**, *94*, 4941−4948.
(3) Bühl, M.; Hirsch, A. *Chem. Rev.* **2001**, *101*, 1153−1183.
(4) Poater, J.; Solà, M. *Chem. Commun.* **2011**, *47*, 11647−11649.
(5) Chen, Z. F.; Wannere, C. S.; Corminboeuf, C.; Puchta, R.; Schleyer, P. V. *Chem. Rev.* **2005**, *105*, 3842−3888.
(6) Fowler, P. W.; Manolopoulos, D. E. *An Atlas of Fullerenes*; Clarendon Press: Oxford, U.K., 1995.
(7) Amsharov, K. Y.; Ziegler, K.; Mueller, A.; Jansen, M. *Chem.—Eur. J.* **2012**, *18*, 9289−9293.
(8) Chen, D. L.; Tian, W. Q.; Feng, J. K.; Sun, C. C. *ChemPhysChem* **2008**, *9*, 454−461.
(9) Tang, S. W.; Feng, J. D.; Sun, L. L.; Wang, F. D.; Sun, H.; Chang, Y. F.; Wang, R. S. *J. Mol. Graphics Modell.* **2010**, *28*, 891−898.
(10) Tan, Y. Z.; Chen, R. T.; Liao, Z. J.; Li, J.; Zhu, F.; Lu, X.; Xie, S. Y.; Li, J.; Huang, R. B.; Zheng, L. S. *Nat. Commun.* **2011**, *2*, 420.
(11) Gogonea, V.; Schleyer, P. v. R.; Schreiner, P. R. *Angew. Chem., Int. Ed.* **1998**, *37*, 1945−1948.
(12) Karadakov, P. B. *J. Phys. Chem. A* **2008**, *112*, 7303−7309.
(13) Wang, W. W.; Dang, J. S.; Zheng, J. J.; Zhao, X. *J. Phys. Chem. C* **2012**, *116*, 17288−17293.
(14) Ōsawa, E.; Ueno, H.; Yoshida, M.; Slanina, Z.; Zhao, X.; Nishiyama, M.; Saito, H. *J. Chem. Soc., Perkin Trans. 2* **1998**, 943−950.
(15) Adamson, A. J.; Holloway, J. H.; Hope, E. G.; Taylor, R. *Fullerene Sci. Technol.* **1997**, *5*, 629−642.
(16) Tan, Y. Z; Xie, S. Y.; Huang, R. B.; Zheng, L. S. *Nat. Chem.* **2009**, *1*, 450−460.
(17) Haddon, R. C. *Acc. Chem. Res.* **1988**, *21*, 243−249.
(18) Rogers, K. M.; Fowler, P. W. *Chem. Commun.* **1999**, 2357−2358.
(19) Wang, W. W.; Dang, J. S.; Zheng, J. J.; Zhao, X.; Nagase, S. *J. Phys. Chem. C* **2013**, *117*, 2349−2357.
(20) Han, X.; Zhou, S. J.; Tan, Y. Z.; Wu, X.; Gao, F.; Liao, Z. J.; Huang, R. B.; Feng, Y. Q.; Lu, X.; Xie, S. Y.; et al. *Angew. Chem., Int. Ed.* **2008**, *47*, 5340−5343.
(21) Shan, G. J.; Tan, Y. Z.; Zhou, T.; Zou, X. M.; Li, B. W.; Xue, C.; Chu, C. X.; Xie, S. Y.; Huang, R. B.; Zhen, L. S. *Chem.—Asian J.* **2012**, *7*, 2036−2039.
(22) Furche, F.; Ahlrichs, R. *J. Chem. Phys.* **2001**, *114*, 10362−10367.
(23) Kovalenko, V. I.; Khamatgalimov, A. R. *Chem. Phys. Lett.* **2003**, *377*, 263−268.